Construction of an Inexpensive, Hand-Held Fundus Camera through Modification of a Consumer "Point-and-Shoot" Camera

Kenneth Tran,[1] *Thomas A. Mendel,*[2,3] *Kristina L. Holbrook,*[2] *and Paul A. Yates*[1,2]

Purpose. To construct a low-cost, easy-to-use, high-image-quality mydriatic fundus camera with "point-and-shoot" operation, and to evaluate the efficacy of this camera to accurately document retinal disease.

Methods. A prototype portable fundus camera was designed by interfacing a novel optical module with a Panasonic Lumix G2 consumer camera. Low-cost, commercially available optics were used to create even illumination of the fundus, providing a 50° retinal field of view. A comparative study assessing the image quality of the prototype camera against a traditional tabletop fundus camera was conducted under an Institutional Review Board (IRB)-approved study.

Results. A stand-alone, mydriatic camera prototype was successfully developed at a parts cost of less than $1000. The prototype camera was capable of operating in a point-and-shoot manner with automated image focusing and exposure, and the image quality of fundus photos was comparable to that of existing commercial cameras. Pathology related to both nonproliferative and proliferative diabetic retinopathy and age-related macular degeneration was easily identified from fundus images obtained from the low-cost camera.

Conclusions. Early prototype development and clinical testing have shown that a consumer digital camera can be inexpensively modified to image the fundus with professional diagnostic quality. The combination of low cost, portability, point-and-shoot operation, and high image quality provides a foundational platform on which one can design an accessible fundus camera to screen for eye disease. (*Invest Ophthalmol Vis Sci.* 2012;53:7600–7607) DOI:10.1167/iovs.12-10449

In 1926, Carl Zeiss Company introduced the first commercially available fundus camera, which offered a 10° retinal field and required manual exposure using flash powder and color film.[1,2] Since then, the capabilities of fundus cameras have improved dramatically to include nonmydriatic imaging, electronic illumination control, automated eye alignment, and high-resolution digital image capture. These improvements have helped make modern fundus photography a standard ophthalmic practice for detecting and documenting retinal disease.[1–3]

Although current fundus cameras have advanced significantly since their introduction, the traditional tabletop optical design has remained largely unchanged.[4,5] Complex optical assemblies in current devices provide high-resolution imaging of the fundus but also require dedicated clinical space and high manufacturing costs. Portable cameras have recently become commercially available, but most remain difficult to use in a hand-held manner and often have substandard image quality, compared to their tabletop counterparts.[6,7]

The commercial field of fundus camera equipment stands in unique contrast to consumer digital camera technology, where personal cameras are becoming ever cheaper, smaller, and easier to use. Although other ophthalmic equipment manufacturers have recently incorporated consumer digital single-lens reflex (DSLR) cameras into their fundus camera designs, they do not make full use of the consumer camera's built-in functions or space-saving design. Traditional fundus camera designs are thus ill suited to leverage the significant cost reductions and technologic advancements of consumer camera technology.

Within the past decade, retinal screening programs for common eye disease, such as diabetic retinopathy and age-related macular degeneration, have experienced rapid growth.[7–10] The expansion of these screening programs into rural, nurse-operated, highly distributed primary care facilities highlights the importance of having access to an inexpensive, portable, easy-to-operate, and high-image-quality fundus camera.[11–13]

Our goal was to create a device capable of imaging the human fundus and documenting retinal pathology with components that cost less than $1000. We also aimed to improve dramatically the ease of use of the device by incorporating common "point-and-shoot" consumer camera technology. A secondary objective was to reduce the design to a portable form factor that would enable remote use of the device in settings such as hospital bed consultations and nursing home facilities. This design would provide a means of acquiring fundus photographs in clinical settings previously inaccessible to tabletop cameras.

In this article, we present the technical modifications needed to transform a consumer digital camera into a mydriatic fundus camera. We also demonstrate the functional feasibility of using such a camera in a variety of clinical settings to produce images of the posterior pole of the eye with pathology detail resolution comparable to that of existing fundus cameras.

Materials and Methods

General Design Description

Human fundus photography is based upon the principle of indirect ophthalmoscopy. A front objective lens is positioned at a working distance of 5 to 50 mm from the front of the eye. This lens is used to

From the [1]Departments of Biomedical Engineering, [2]Ophthalmology, and [3]Pathology, University of Virginia, Charlottesville, Virginia.

Supported by the UVa-Coulter Translational Partnership Grant (GF11938), Ivy Foundation of Charlottesville Research Grant (DR-02314), and National Institutes of Health (NIH) Grants T32 GM08715 (TAM) and K08 GC11897 (PAY).

Submitted for publication June 22, 2012; revised September 2, 2012; accepted October 2, 2012.

Disclosure: **K. Tran**, RetiVue, LLC (I, E, S), P; **T.A. Mendel**, None; **K.L. Holbrook**, None; **P.A. Yates**, RetiVue, LLC (I, E, S), P

Corresponding author: Paul A. Yates, Department of Ophthalmology, PO Box 801375, Charlottesville, VA 22908; pyates@virginia.edu.

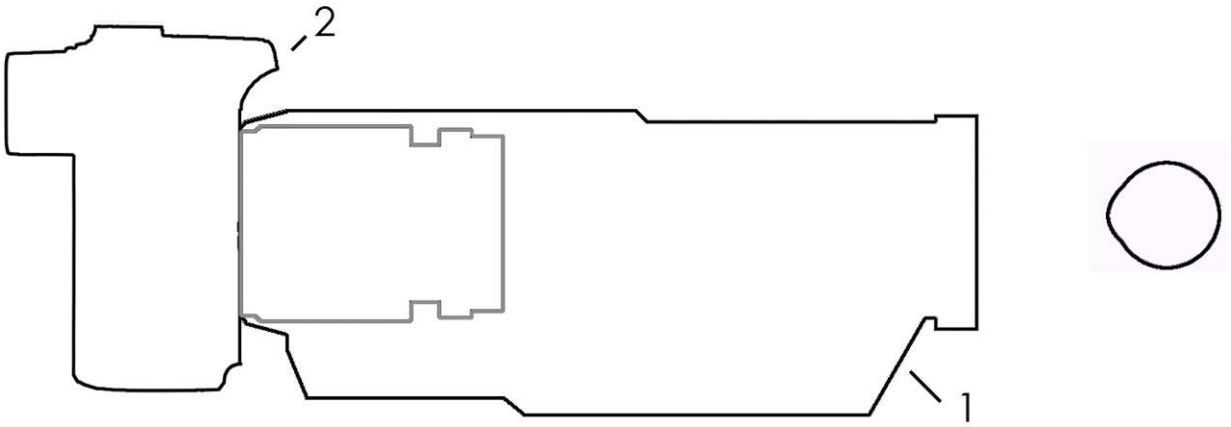

Figure 1. General diagram of the prototype low-cost portable fundus camera. The design is separated into two modules: (**1**) an attachment housing optical components and (**2**) an off-the-shelf consumer digital camera.

simultaneously relay light rays toward the eye, collect the reflected light, and also provide a magnified view of the fundus.

We designed an optical system based upon this imaging principle that comprised a two-part modular system: an optical attachment that integrates all of the optical components necessary to produce an image of the fundus (Fig. 1, module 1), and a camera that was used to compose, capture, and store an image of the fundus (Fig. 1, module 2). A schematic diagram of the components within the optical attachment module is shown in Figure 2. All camera components were integrated within a custom housing designed by using Rhino3D software (McNeel, Seattle, WA) and built by using rapid stereolithography prototyping techniques (Metro Rapid Prototyping, Noblesville, IN). The final prototype of the fundus camera measures approximately 245×95×75 mm. Detailed descriptions of the fundus camera components are provided in subsequent sections (see Supplementary Material and Supplementary Table S1 for detailed component list and cost breakdown, http://www.iovs.org/lookup/suppl/doi:10.1167/iovs.12-10449/-/DCSupplemental).

Fundus Imaging

The primary function of the optical attachment is to provide the imaging path (Fig. 2, module 1) necessary for the consumer camera to capture an image of the fundus. A 22-diopter (D) indirect ophthalmic lens (Ocular Instruments, Bellevue, WA) (Fig. 2, module 4) was used as the front objective lens of the fundus camera. This lens was selected owing to a number of favorable characteristics including: a 60° field of view, a large clear aperture of 52 mm for improved light transmission, and advanced antireflection coatings. A Panasonic Lumix G2 (Panasonic Corporation, Kadoma, Osaka, Japan) was selected as the camera back (Fig. 1, module 2). This camera has a number of desirable features including large 12-megapixel (MP) complementary metal-oxide-semiconductor (CMOS) sensor, rapid automatic focus and exposure capabilities, hot-shoe adapter, Live-View imaging, interchangeable lensing, and built-in image stabilization.

The front objective lens, which operates with a working distance of 39 mm, was placed co-axially from the front lens of the consumer

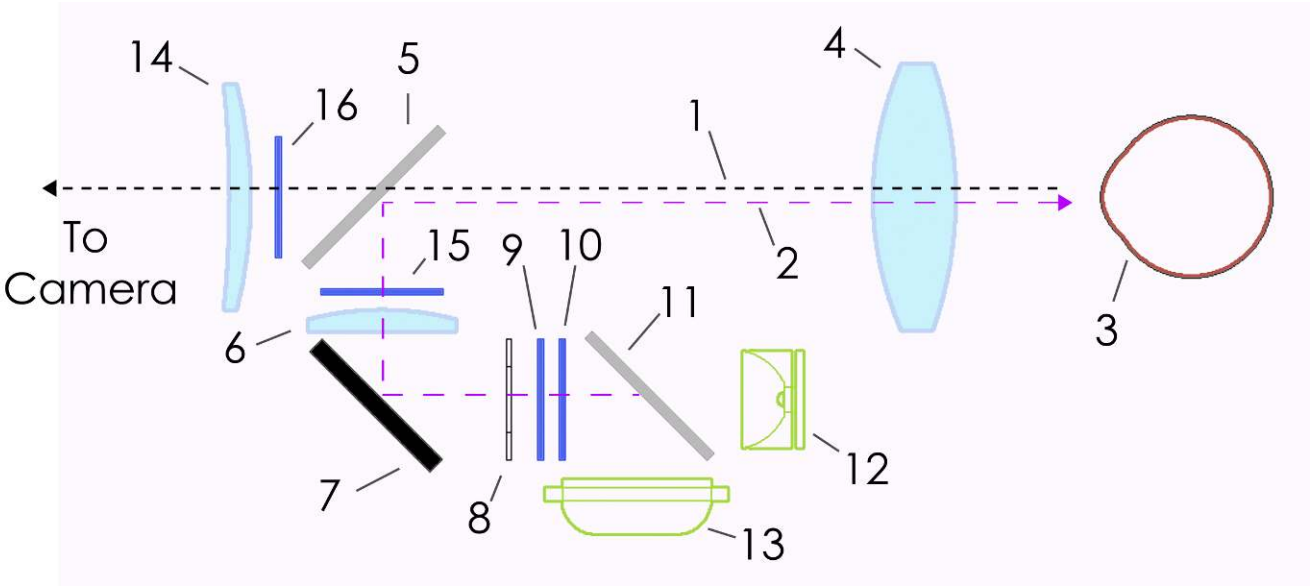

Figure 2. Optical configuration of the prototype camera (distances between components are approximated). A shared, (**1**) co-axial imaging and (**2**) illumination path was used by coupling with a (**5**) beam splitter. Diagram components are specified as follows: (**3**) human eye, (**4**) front objective lens, (**5**) beam splitter, (**6**) condensing lens, (**7**) mirror, (**8**) image mask, (**9**) holographic diffuser, (**10**) UV filter, (**11**) beam splitter, (**12**) visible LED unit, (**13**) xenon flash tube, (**14**) macro lens, (**15**) linear polarizer, and (**16**) analyzer polarizer. This configuration allows a reflection-free, 50° field of view of the fundus in an external housing that can be attached to a consumer digital camera that maintains hand-held, point-and-shoot operation.

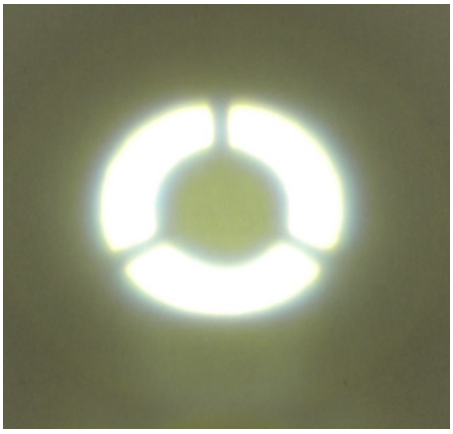

FIGURE 3. Annular illumination pattern used by the fundus camera. A 5.1-mm clear central aperture allows for corneal reflection-free imaging of the fundus.

camera. In our prototype, the distance between the objective lens and the Panasonic lens was 125 mm. Screw-in macro lenses (Schneider Optics, Hauppauge, NY) (Fig. 2, module 14) were attached to the Panasonic camera's front lens to increase close focusing ability, with the zoom set to 35 mm. This configuration allows a focused image of the retina formed by the front objective lens to fill the entire image sensor of the camera. In addition, an internal circular image baffle was designed as part of the housing, which functioned to crop the field of view to 50°.

Fundus Illumination

Proper illumination of the retinal field was obtained by focusing an annular illumination pattern co-axially onto the corneal surface of the eye (Fig. 3). An annular-patterned illumination scheme is commonly used in existing fundus camera design and provides the camera with a clear central imaging aperture. In our camera, an annulus of light was created by placing a donut-shaped image mask with an optically opaque central aperture (Fig. 2, module 8).[4,5] The dimensions of the annulus were optimized with an inner diameter (ID) of 5.0 mm and an outer diameter (OD) of 7.0 mm, corresponding to the average range of pupil diameters of a fully dilated human eye.[14] The annulus is focused 52 mm from the front objective lens with a beam angle of 44° and beam waist of 7.0/5.0 mm (OD/ID). We have found that this configuration provides a bright, near-lambertian illumination pattern on the retina that is free of corneal reflections.

A continuous illumination source for image composition and focusing was provided by a light emitting diode (LED) with a color temperature of 2700°K (Luxeon Star, Brantford, Ontario, Canada) (Fig. 2, module 12). The LED was prebuilt with a 10° condensing lens and was powered by a 1000-mA BuckPuck current driver (Luxeon Star) using four AA batteries. Although this LED source could be used for final image capture, the low optical power would necessitate slow exposure settings. Therefore, an external xenon flash (YongNuo, Futian District, Shenzhen, China) (Fig. 2, module 13) was incorporated into the design to allow high shutter speed exposures. This feature decreases image noise and eliminates artifacts from subject eye drift or camera shake.

A brief description of the illumination ray path (Fig. 2, module 2) from source origin to the eye is as follows: light originating from the LED and xenon flash are combined by using a 50/50 beam splitter (Edmund Optics, Barrington, NJ) (Fig. 2, module 11), passed through a UV-blocking film (Edmund Optics) (Fig. 2, module 10), and projected toward a holographic diffuser (Luminit, Torrance, CA) (Fig. 2, module 9). The near-lambertian emergent light is then directed toward the annular image mask to produce an annular bundle of light. This light is vertically reflected by a 45° mirror (Edmund Optics) (Fig. 2, module 7), passed through a condensing lens (Edmund Optics) (Fig. 2, module 6), and projected to a second 50/50 beam splitter (Fig. 2, module 5). The image of the illuminated annulus, now co-axial with the imaging path (Fig. 2, module 1), is relayed through the front objective lens (Fig. 2, module 4) and focused on the corneal surface.

Image Artifact Reduction

Although the two-lens optical system described above can capture properly focused and composed fundus images, a significant consequence of a simplified optical train is the existence of optical aberrations. As a result, fundus images from the present camera suffer from image artifacts, primarily lens reflections off the center of the front objective lens. To reduce these reflections, a method of cross-polarization was adapted. Cross-polarization is a commonly used macrophotography technique and has also seen limited use in the ophthalmic field.[15–19]

A pair of perpendicularly crossed linear polarizers (Edmund Optics) (Fig. 2, modules 15, 16) was introduced at two locations in the optical path. The first polarizer was placed between the condensing lens (Fig. 2, module 6) and the imaging beam splitter (Fig. 2, module 5). This polarizer absorbs incoming light from the illumination source and only transmits light that is parallel to its polarization axis. The second polarizer is placed before the camera's zoom lens and acts as an analyzing filter, only transmitting light to the camera sensor, which has a polarization axis perpendicular to the illumination rays emerging from the first polarizer. Polarized light rays reflected from the retinal surface become randomized and are thus able to pass through the analyzing polarizer. However, light reflected off hard manufactured surfaces, such as glass, retains the original polarization state and therefore is eliminated by the analyzing polarizer.

Camera Operation

Operation of the constructed fundus camera is similar to the operation of a common consumer camera. Focal length, shutter speed, aperture, and International Organization for Standardization (ISO) were preset to 35 mm, 1/160 s, f/9, and 400, respectively. The user turns on the observation illumination source on the optical attachment. The front objective lens is then aimed at the eye. Image composition and autofocusing is performed on the camera's built-in LCD screen. We found that proper focus on the retina can be obtained most readily by moving the focusing area of the camera over the optic nerve. The image contrast resulting from the optic disc and surrounding vasculature allows the camera's contrast-based autofocusing algorithms to lock accurate focus. A fundus image is then acquired by depressing the shutter button. As such, a point-and-shoot operation sequence was maintained.

Ocular Safety Assessment

Preliminary light hazard assessment consisted of measuring total radiant energy and effective blue-light and UV-A radiant exposure. Primary radiometric measurements of both LED and xenon light sources were made with a calibrated Gentec Ultra-UP Radiometer and XLP12-1S-H2-D0 detector (GenTec-EO, Quebec, QC, Canada) with a spectral range between 190 nm and 11 μm. These measurements were checked by using a calibrated ILT 1400A radiometer/photometer with SEL240, SEL033-F No. 14,299, and SEL033-UVA No. 28,246 detectors (International Light Technologies, Peabody, MA) to measure UV, 380- to 1000-nm, and 315- to 400-nm irradiance, respectively. All measurements were taken where the beam diameter filled the circular entrance aperture of the detector. In most cases, the detector was placed 10 to 15 mm from the focal point of the annulus. Lamp safety was determined by applying standard criteria for photobiological safety of lamps and ophthalmic instruments.[20–23]

Figure 4. Front and rear depictions of the prototype low-cost fundus camera. The design uses a consumer camera for intuitive, point-and-shoot operation.

Clinical Testing Protocol

Clinical testing of the prototype fundus camera was carried out under an Institutional Review Board (IRB)-approved clinical study at the University of Virginia Medical Center and in full compliance with the Declaration of Helsinki. Informed consent was obtained from each subject ($n = 6$ eyes in 6 patients) after explanation of the nature of the camera study and all risks associated with participation. Mydriatic fundus photography was carried out with pharmacologic pupil dilation by using 1% tropicamide and 2.5% phenylephrine. The study method consisted of taking successive unilateral photographs with the prototype camera and a TRC-50EX mydriatic camera (TopCon Medical Systems, Tokyo, Japan). Subjects were randomized to the order in which photos were taken from each camera. This allowed for direct pathology identification comparisons between the two fundus cameras under subject-replicated refractive errors and media opacities. An additional IRB-approved study was conducted for fundus photography in clinical hospital consultation settings ($n = 2$ eyes in 2 patients), where tabletop TopCon fundus photos were impossible to obtain. All images acquired were equivalently postprocessed by using Adobe Photoshop (Adobe, San Jose, CA), with uniform adjustments to image contrast, levels, brightness, and sharpness filtering applied across the entire image.

Results

Beam and Light Exposure Characteristics

The subject, when properly positioned for fundus photography, experiences uniform retinal illumination over a 46° to 50° field. The exact angular field of illumination varies as a function of pupil entrance diameter. The spread of the emitted beam of light was fixed at 50° for a 19-mm-diameter beam. This illuminates a 14- to 16-mm-diameter area of the retina.

Total radiant power for the LED source was calculated to be 0.25 mW, corresponding to a radiant exposure of 0.13 mJ/cm^2. The total radiant exposure of the xenon flash lamp was found to be 0.43 mJ per pulse with a pulse duration of between 33 and 125 μs, corresponding to a radiant exposure of approximately 1.0 uJ/cm^2. According to the American Conference of Governmental Industrial Hygienists (ACGIH)/International Commission on Non-Ionizing Radiation Protection (ICNRIP) exposure guideline of 3 mJ/cm^2, more than 3000 flashes would be required during an 8-hour period to exceed the daily limit.[20] UV-B exposure totaled no greater than 0.01 μW/cm^2 for the LED source, and less than 1 μJ/cm^2 for the xenon flash. UV-A irradiance values were calculated to be on the order of 1 μW/cm^2 for the LED and less than 5 μJ/cm^2 for the xenon flash. Similarly, these values are at least 100-fold below safety limits. These measurements did not exceed the long-term total irradiance limit of 10 mW/(cm^2·sr) as specified in American National Standards Institute (ANSI) code RP-27.3-07, and accordingly, the LED and xenon flash sources can be classified as in exempt risk group (values summarized in Supplementary Table S2; see Supplementary Material and Supplementary Table S2, http://www.iovs.org/lookup/suppl/doi:10.1167/iovs.12-10449/-/DCSupplemental).[20] Anecdotally, a number of subjects commented on the relative decrease in brightness from the portable camera compared to other tabletop cameras, which significantly improved subject comfort during photography sessions.

Portable Fundus Imaging

The finished fundus camera prototype (Fig. 4) was able to be used in a hand-held and portable manner with the subject sitting down in a reclined head position. We found that the camera was most stable when operated while the user was standing. Both hands were used to stabilize the camera, with the first holding the Panasonic camera's built-in rubber grip and the other grasping the front lens with the index finger and thumb, while using other fingers to stabilize across the subject's forehead. This hand provided a stable pivoting point to vary axial, horizontal, and vertical distances from the subject's eye from which proper alignment could be easily achieved with practice. In most cases, the front lens of the camera was positioned between 40 to 45 mm away from the subject's eye, depending upon variances in refractive power.

We found that both optic nerve and macula-centered images could be obtained, but this requires a certain degree of subject co-operation. Image acquisition times ranged from 10 to 25 seconds for each photo. Subject variability in media opacities, dilated pupil size, and reflectivity of the fundus were found to significantly affect the ability to quickly and successfully acquire fundus images, often resulting in low, partial, or vignette exposure of the fundus. For these reasons, an average of two to four photos were taken per eye to ensure satisfactory quality for clinical diagnosis. Overall, 22 of 26 photos (85%) taken were judged sufficient for clinical diagnosis.

Reflection Elimination

Preliminary laboratory testing with the constructed fundus camera demonstrated the importance of image artifact and reflection elimination. Fundus photographs obtained with nonpolarized illumination resulted in a central lens reflection located over the foveal region in a macular-centered image, potentially obscuring details in this important anatomic region (Fig. 5A). This can be attributed to internal reflections from the image mask reflecting off of the front lens surface and is a fundamental consequence of many standard fundus camera designs.

A number of optical and digital methods may be used for reducing the central lens reflection, including placing a small black dot in the center of the front condensing lens (Fig. 2, module 4), using a light baffle, placing the illumination system (Fig. 2, modules 5–12) outside of the camera between the eye (Fig. 2, module 3) and front condensing lens, or taking two photos with overlapping fields of view and digitally subtracting the reflection. We found that the most straightforward approach with best photographic result was to introduce polarizing filters (Fig. 2, modules 15, 16) into the optical path, with the filters oriented at 90° to one another to achieve cross polarization. The addition of polarizing filters into the optical system results in a dramatically reduced central lens reflection to a size and brightness equivalent to that of other commercial

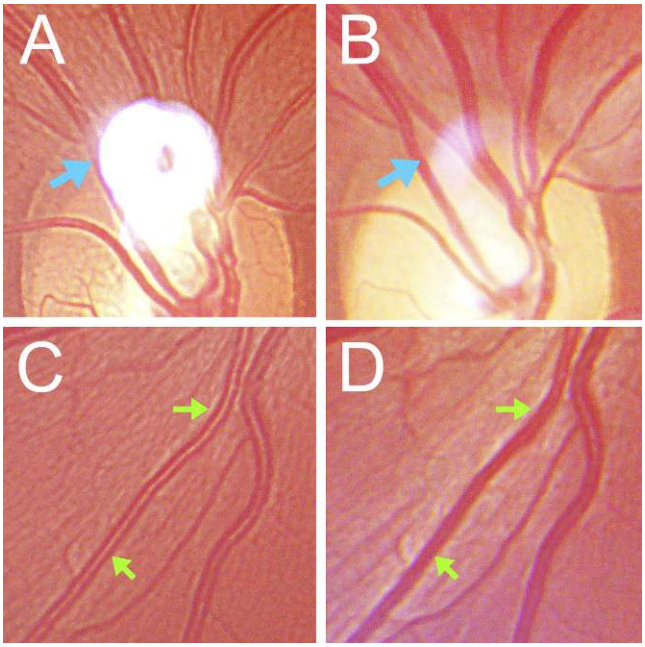

Figure 5. Effect of image polarization on fundus image quality. (**A**) Unpolarized fundus image with prominent central lens reflection (*teal arrow*). (**B**) Polarized fundus image and dramatic reduction of central lens reflection (*teal arrow*). (**C**) Unpolarized fundus image with visualization of reflectivity sheen from the blood vessels (*green arrow*) and nerve fiber layer. (**D**) Polarized fundus image demonstrating marked reduction in blood vessel sheen reflectivity (*green arrow*). All images were obtained as optic nerve–centered images on the same subject.

fundus cameras (Fig. 5B). Polarizing the retinal field also results in reduction in corneal haze from media opacities and, as a result, improves image detail definition and contrast.

A consequence of image polarization is a loss of reflectivity from highly refractive surfaces such as the internal limiting membrane and nerve fiber layer (Figs. 5C, 5D). These findings were supportive of prior studies using cross-polarization for viewing the fundus, including ophthalmoscopy; specular reflection biomicroscopy; and optic disc, anterior segment, and nerve fiver layer fundus photography. These studies have shown that cross-polarization enhances the ability to image eyes with cataract or vitreous haze, and accentuates defects in the nerve fiber layer.[15–18] Cross-polarization also improves visualization of subretinal details, including exudates and drusen. Given the intended use of this camera for retinal screening of diabetic retinopathy and macular degeneration, we believe this is a favorable compromise.

Of note, the employed polarization scheme resulted in a theoretical 75% reduction in available light reaching the camera sensor. However, we found that this can be compensated by increasing output from the flash lamp and doubling the exposure ISO from 200 to 400.

Image Analysis and Clinical Documentation

The point-and-shoot fundus camera was capable of obtaining co-axial images of the fundus with a field of view of approximately 50°. The consumer camera captured a 7.8-MP image as measured by the total pixel area contained within the circular retinal area. Total image dimensions measured 3158 × 3158 pixels, corresponding to 57 pixels per retinal field degree. These measurements exceed the image resolution benchmarks of 6 MP and 30 pixels per degree set forth by the United Kingdom's National Health Service for effective retinopathy screening and detection of diabetic retinopathy (DR)-related pathology.[24]

A unilateral clinical comparison photograph obtained by using the prototype fundus camera and a commercial tabletop camera validated the ability of the camera to accurately document retinal pathology. As demonstrated in this image, the prototype camera was capable of imaging the retina with comparable quality to the commercial equivalent (Fig. 6). Indeed, all of retinal pathology, including micro-aneurysms, dot blot hemorrhages, soft drusen, and laser scarring, could be equally visualized and identified with the hand-held prototype. As with commercial fundus cameras, stereo pair photography is also possible, which can facilitate identification of optic nerve cupping as well as retinal and subretinal pathology (Fig. 7). Similar results were obtained from each of the eight subjects involved with the study, wherein an accurate diagnosis of retinal disease (or lack thereof) was made across replicate unilateral comparison photographs. The camera was

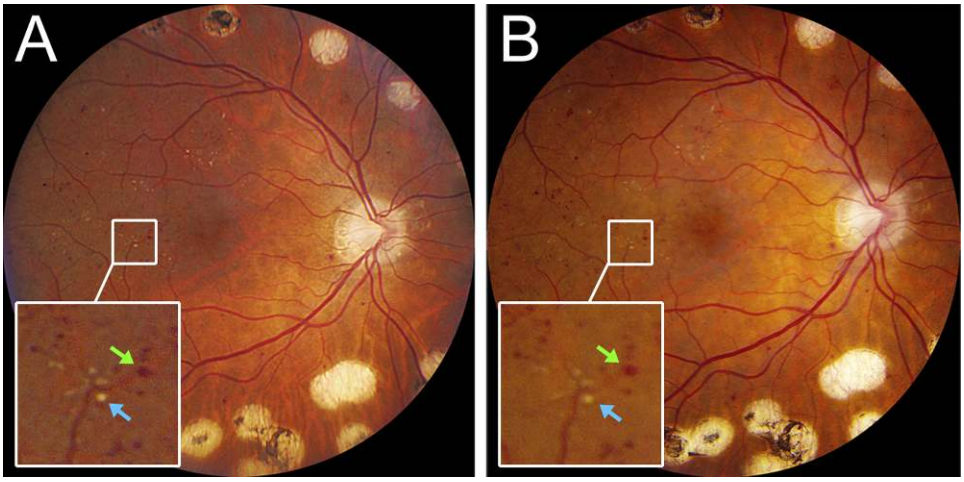

Figure 6. Unilateral comparison photographs taken with (**A**) the hand-held prototype camera and (**B**) a commercial TopCon TRC-50EX camera. Right eye images show a subject suffering from diabetic retinopathy, with significant dot blot hemorrhaging (*green arrows*), exudates (*teal arrows*), and laser scarring post ablation therapy. One-hundred percent of the retinal pathology identified with the commercial camera could be equally identified with the low-cost portable camera.

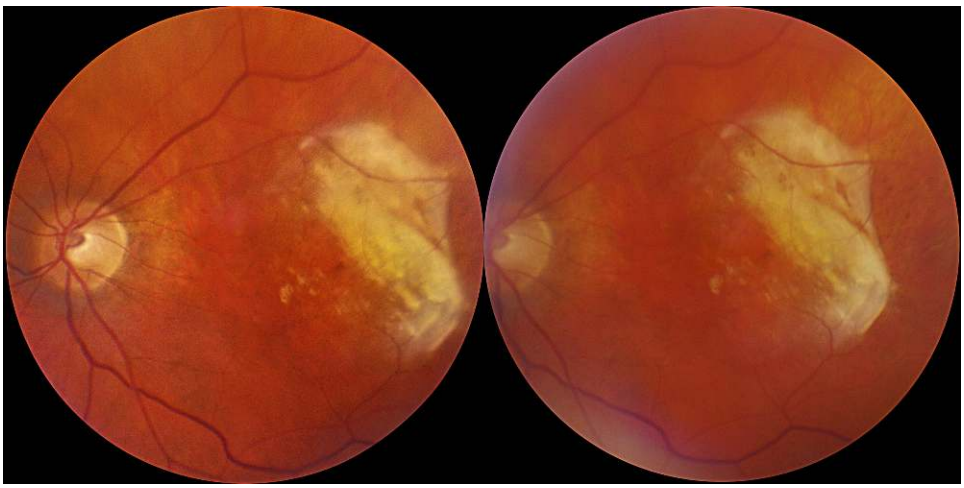

Figure 7. Stereo pair images obtained with the prototype camera, demonstrating exudative AMD with subretinal fibrosis.

also able to visualize regions of geographic atrophy, vitreomacular traction, and signs of wet AMD (Fig. 8).

Discussion

We reported that a point-and-shoot retinal camera can be inexpensively built around a consumer digital camera and that such a camera is capable of performing high-resolution 50° mydriatic retinal imaging in a compact and portable form factor. We believe that the described system offers specific practical advantages over currently available tabletop fundus cameras and other portable ophthalmic imaging devices.

First, our camera leverages recent advancements in consumer camera technology, including, but not limited to,

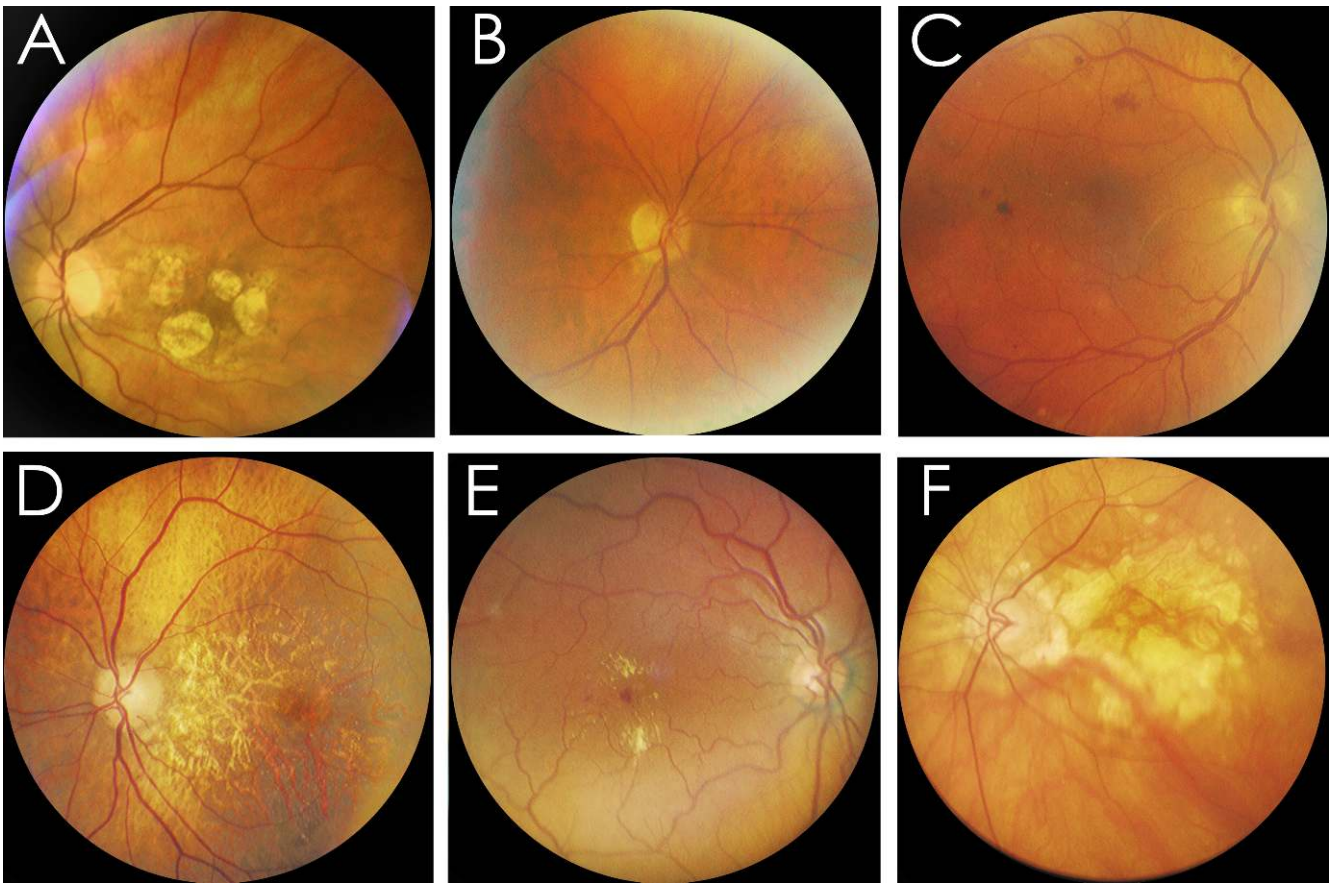

Figure 8. Right and left eye fundus photographs obtained with the low-cost, point-and-shoot camera. The unilateral fundus photographs of the study participants show a variety of retinal pathology, including (**A**) geographic atrophy, (**B**) a healthy fundus, (**C**) background diabetic retinopathy with exudates and vitreomacular traction, (**D**) geographic atrophy with drusen, (**E**) diabetic retinopathy with exudate and dot blot hemorrhage, and (**F**) geographic atrophy.

large low-noise image sensors, live view imaging, image stabilization, and secure digital (SD)-card storage. In addition, retinal pathology can be immediately identified after image capture by using the camera's LCD display. The independent modular design also allows one to upgrade the camera back as consumer camera technology continues to evolve. Indeed, we have successfully retrofitted the front-end optical module onto other consumer cameras, including the Canon G12 (Canon, Lake Success, NY) and Kodak M750 (Kodak, Rochester, NY). However, the smaller charge coupled device (CCD) sensors found on these cameras result in loss of image detail and increased noise as compared to the larger CMOS sensor found in the Panasonic Lumix G2 camera.

Second, cost-conscious efforts were made throughout the design and construction of the point-and-shoot camera, with a total component parts cost of less than $1000. We significantly reduced hardware costs by foregoing a compound front objective lens and custom multistage optical train, instead using a 22-D ophthalmic indirect lens and simpler, commercially available optics. However, the prototype build cost does not necessarily imply the retail price for a commercial version of this device, as many variables are involved in determining this. Choice of a less expensive camera back and production of the camera in larger volumes would both serve to substantially decrease parts costs, while the traditional medical device markup of 2 to 3 times production costs would serve to increase the final retail price.

While the camera has exceeded our initial expectations in limited use, we make no formal claims of equivalency or efficacy to commercial tabletop fundus cameras, as a formal clinical study has yet to be performed. It is important to note that the present study excluded subjects with significant ocular opacities. A subsequent study should consist of a larger, more variable subject cohort with image evaluation performed by blinded, independent graders. In addition, other parameters, such as image acquisition time and percentage of gradable images, must be compared to existing commercial cameras. Such a study would be necessary to truly demonstrate clinical equivalency with commercial fundus cameras. Nonetheless, we hope that in the future this camera platform can be a suitable replacement for traditional tabletop photography in the primary care setting, particularly for use in screening for common eye diseases such as diabetic retinopathy.

Although the prototype camera may be sufficient as is for screening photography, a number of improvements could be made to improve usability in the clinic. Currently, the user is required to place the "focus box" of the camera directly over the high-contrast area of the optic nerve and surrounding trunk vessels in order to obtain accurate focus. After using this method, most images obtained in the clinical study were found to be properly in focus. A small percentage of photos, however, were affected by slight image blur and soft focus. This was likely due to individual variations in media opacity. It may be possible to improve the focusing method to account for these subject variations by fine-tuning image contrast and focus point settings in camera. There is also currently no method of eye fixation on the camera. We found that patients with cognitive impairments had difficultly keeping their eye steady without a fixation target, often resulting in out-of-focus and misaligned fundus images. To address this issue, a flexible external fixation target can be affixed to the exterior housing. Finally, alignment of the camera with the eye to obtain suitable retinal photographs relies on operator expertise, and this could be improved with some means to better determine proper alignment with the eye, as found on commercial tabletop devices.

Perhaps the most important limitation of the current camera is the need for pharmacologic mydriasis. To conduct efficient screening programs, one must provide the ability to image the retina nonmydriatically.[7,12,13] The current camera cannot be used effectively without pharmacologic dilation, as the brightness of the alignment LED is significant enough to cause virtually all pupils to constrict below 3 mm. It may be possible to modify the camera and underlying optics of the optical attachment to image in the infrared spectrum, and therefore enable nonmydriatic use. This would involve modifying the image sensor to visualize infrared wavelengths, as well as replacing the existing visible spectrum LED with an 850-nm LED. Such an arrangement would allow the user to view the external eye and fundus in infrared in a similar manner as other commercial nonmydriatic fundus cameras.

The image quality of the camera may be further improved by coupling a highly sensitive scientific-grade imaging sensor to a front objective lens with shorter working distances to the eye. These changes would substantially improve light gathering capability while decreasing the size and weight of the current prototype fundus camera. However, this approach has several disadvantages. First, using a separate imaging sensor would require much higher design complexity involving custom user interface integration and software, instead of directly leveraging a consumer product platform. Second, shorter working distances in close proximity to the patient's eye would result in patient discomfort as well as greater potential for operator error during alignment.

In conclusion, a portable, point-and-shoot retinal camera can be constructed by using a novel combination of commercial optics and a consumer digital camera with a component cost inferior to $1000. The constructed prototype camera was able to compose, capture, and store images all in a single compact, hand-held device. Most importantly, nonophthalmic medical personnel, such as nurses and administrative staff, should be able to easily use this camera after only minimal training. The combination of these three features in a retinal camera—low cost, portability, and ease of use—provides a foundational platform from which a revolutionary screening camera can potentially be designed.

Acknowledgments

The authors thank Shayn Peirce-Cottler, Brendan Zotter, and David Kao (University of Virginia, Charlottesville, Virginia) for reviewing this manuscript; David Sliney for assisting with retinal hazard assessment; and Alan Lyon of the University of Virginia Department of Ophthalmology for technical assistance.

References

1. Mann WA. History of photography of the eye. *Sur Ophthalmol*. 1970;15:179–189.
2. Van Cader TC. History of ophthalmic photography. *J Ophthalmic Photogr*. 1978;17–19.
3. Bennett TJ, Barry CJ. Ophthalmic imaging today: an ophthalmic photographer's viewpoint—a review. *Clin Experiment Ophthalmol*. 2009;37:2–13.
4. Gutner R, Miller D. Inside the fundus camera. *Ann Ophthalmol*. 1983;15:13–16.
5. DeHoog E, Schwiegerling J. Fundus camera systems: a comparative analysis. *Appl Opt*. 2009;48:221–228.
6. Gliss C, Parel JM, Flynn JT, Pratisto H, Niederer P. Toward a miniaturized fundus camera. *J Biomed Opt*. 2004;9:126–131.
7. Yogesan K, Constable IJ, Barry CJ, Eikelboom RH, McAllister IL, Tay-Kearney ML. Telemedicine screening of diabetic retinopathy using a hand-held fundus camera. *Telemed J*. 2000;6:219–223.

8. Cheung N, Mitchell P, Wong TY. Diabetic retinopathy. *Lancet*. 2010;376:124–136.
9. Mohamed Q, Gillies MC, Wong TY. Management of diabetic retinopathy: a systematic review. *JAMA*. 2007;298:902–916.
10. Saligan LN. Preventing diabetic retinopathy in primary care. *Nurse Pract*. 2008;33:46–47.
11. Klein R, Meuer SM, Moss SE, Klein BE, Neider MW, Reinke J. Detection of age-related macular degeneration using a non-mydriatic digital camera and a standard film fundus camera. *Arch Ophthalmol*. 2004;122:1642–1646.
12. Taylor CR, Merin LM, Salunga AM, et al. Improving diabetic retinopathy screening ratios using telemedicine-based digital retinal imaging technology: the Vine Hill study. *Diabetes Care*. 2007;30:574–578.
13. Askew D, Schluter PJ, Spurling G, et al. Diabetic retinopathy screening in general practice: a pilot study. *Aust Fam Physician*. 2009;38:650–656.
14. Bradley JC, Bentley KC, Mughal AL, Bodhireddy H, Brown SM. Dark-adapted pupil diameter as a function of age measured with the NeurOptics pupillometer. *J Refract Surg*. 2011;27:202–207.
15. Fariza E, Jalkh AE, Thomas JV, O'Day T, Peli E, Acosta J. Use of circularly polarized light in fundus and optic disc photography. *Arch Ophthalmol*. 1988;106:1001–1004.
16. Fariza E, O'Day T, Jalkh AE, Medina A. Use of cross-polarized light in anterior segment photography. *Arch Ophthalmol*. 1989;107:608–610.
17. Sommer A, Kues HA, D'Anna SA, Arkell S, Robin A, Quigley HA. Cross-polarization photography of the nerve fiber layer. *Arch Ophthalmol*. 1984;102:864–869.
18. Peli E. Circular polarizers enhance visibility of endothelium in specular reflection biomicroscopy. *Arch Ophthalmol*. 1985;103:670–672.
19. Evans JN. Polarized light attachment for ophthalmoscopy. *Trans Am Ophthalmol Soc*. 1936;34:113–117.
20. Delori FC, Webb RH, Sliney DH; American National Standards Institute. Maximum permissible exposures for ocular safety (ANSI 2000), with emphasis on ophthalmic devices. *J Opt Soc Am A Opt Image Sci Vis*. 2007;24:1250–1265.
21. Sliney DH. Ocular injury due to light toxicity. *Int Ophthalmol Clin*. 1988;28:246–250.
22. Sliney DH. Optical radiation safety of medical light sources. *Phys Med Biol*. 1997;42:981–996.
23. Sliney DH. Radiometry and laser safety standards. *Health Phys*. 1989;56:717–724.
24. National Health Service. Essential elements to developing a diabetic eye screening programme. Available at: http://diabeticeye.screening.nhs.uk/workbook. Published January 19, 2012. Accessed May 5, 2012.